

# Recovery potential of the world's coral reef fishes

M. Aaron MacNeil<sup>1,2,3</sup>, Nicholas A. J. Graham<sup>3</sup>, Joshua E. Cinner<sup>3</sup>, Shaun K. Wilson<sup>4,5</sup>, Ivor D. Williams<sup>6</sup>, Joseph Maina<sup>7,8</sup>, Steven Newman<sup>9</sup>, Alan M. Friedlander<sup>10,11</sup>, Stacy Jupiter<sup>8</sup>, Nicholas V. C. Polunin<sup>9</sup> & Tim R. McClanahan<sup>8</sup>

**Continuing degradation of coral reef ecosystems has generated substantial interest in how management can support reef resilience<sup>1,2</sup>. Fishing is the primary source of diminished reef function globally<sup>3–5</sup>, leading to widespread calls for additional marine reserves to recover fish biomass and restore key ecosystem functions<sup>6</sup>. Yet there are no established baselines for determining when these conservation objectives have been met or whether alternative management strategies provide similar ecosystem benefits. Here we establish empirical conservation benchmarks and fish biomass recovery timelines against which coral reefs can be assessed and managed by studying the recovery potential of more than 800 coral reefs along an exploitation gradient. We show that resident reef fish biomass in the absence of fishing ( $B_0$ ) averages  $\sim 1,000 \text{ kg ha}^{-1}$ , and that the vast majority (83%) of fished reefs are missing more than half their expected biomass, with severe consequences for key ecosystem functions such as predation. Given protection from fishing, reef fish biomass has the potential to recover within 35 years on average and less than 60 years when heavily depleted. Notably, alternative fisheries restrictions are largely (64%) successful at maintaining biomass above 50% of  $B_0$ , sustaining key functions such as herbivory. Our results demonstrate that crucial ecosystem functions can be maintained through a range of fisheries restrictions, allowing coral reef managers to develop recovery plans that meet conservation and livelihood objectives in areas where marine reserves are not socially or politically feasible solutions.**

There is widespread agreement that local and global drivers need to be addressed to reduce the degradation of coral reef ecosystems worldwide<sup>1,2</sup>. Numerous reef fisheries are so severely overexploited that critical ecosystem functions such as herbivory and predation are at risk<sup>3–5</sup>. Attempts to rebuild reef fish abundances and associated functions require clear timeframes over which assemblages can be restored, and viable management alternatives, such as marine reserves or gear restrictions, that promote recovery. Here we develop the first empirical estimate of coral reef fisheries recovery potential, compiling data from 832 coral reefs across 64 localities (countries and territories; Fig. 1a) to: (1) estimate a global unfished biomass ( $B_0$ ) baseline—that is, the expected density of reef fish on unfished reefs ( $\text{kg ha}^{-1}$ ); (2) quantify the rate of reef fish biomass recovery in well-enforced marine reserves using space-for-time substitution; (3) characterize the state of reef fish communities within fished and managed areas in terms of depletion against a  $B_0$  baseline; (4) predict the time required to recover biomass and ecosystem functions across the localities studied; and (5) explore the potential returns in biomass and function using off-reserve management throughout the broader reefscape.

We used a Bayesian approach to estimate jointly  $B_0$  as the recovery asymptote from well-enforced marine reserves (where fishing is effectively prohibited; Fig. 1b) and the average standing biomass of unfished remote areas more than 200 km from human settlements (Fig. 1c). We first used a space-for-time analysis of recovery in well-enforced marine reserves that varied in age and controlled for available factors known to influence

observed fish biomass, including local net primary productivity, the percentage of hard coral cover, water depth, and reserve size<sup>6</sup> (Fig. 1b). We then modelled  $B_0$  by linking this recovery data with prior information<sup>4</sup> on  $B_0$  and biomass from remote reefs (Fig. 1c), an approach that explicitly assumes that marine reserves have the potential to recover to such levels in the absence of complicating factors, such as poaching or disturbance, and are of appropriate size<sup>6</sup>. Globally, expected  $B_0$  for diurnally active, resident reef fish was 1,013 (963, 1469)  $\text{kg ha}^{-1}$  (posterior median (95% highest posterior density intervals)), with a biomass growth rate ( $r_0$ ) of 0.054 (0.01, 0.11) from an estimated initial biomass in heavily fished reefs of 158 (43, 324)  $\text{kg ha}^{-1}$  (Fig. 1). The wide uncertainty in absolute  $B_0$  reflected variability in average biomass among remote localities (from  $\sim 500$  to  $4,400 \text{ kg ha}^{-1}$ ; log-scale coefficient of variation = 0.08; geometric coefficient of variation = 0.61) as well as differences in productivity, hard coral cover, and atoll presence among reefs (Extended Data Fig. 1). We found no evidence of data provider bias (Extended Data Fig. 2) and model goodness-of-fit showed no evidence of lack of fit (Bayesian  $P = 0.521$ ; Extended Data Fig. 3).

The status of reef fish assemblages on fished reefs against a  $B_0$  baseline varied considerably by locality and whether there were management restrictions on fishing activities. Fished reefs (those that lacked management restrictions) spanned a wide range of exploitation states, from heavily degraded in the Caribbean and western Pacific, to high-biomass in the remote but inhabited Pitcairn and Easter Islands (Fig. 2a). Although previous studies have assessed how global reef fish yields relate to human population density<sup>7</sup>, we characterize, for the first time, the state of fished reefs against an empirical baseline. Of concern was that more than a third of the fished reefs sampled had biomass below 0.25  $B_0$ , a point below which multiple negative ecosystem effects of overfishing have been shown to occur in the western Indian Ocean<sup>7</sup>. Only two localities, in Papua New Guinea and Guam, were at or near 0.1  $B_0$ , a fisheries reference point assumed to indicate collapse<sup>8</sup>. Reef fish assemblages fared far better when fishing activities were restricted in some way, including limitations on the species that could be caught, the gears that could be used, and controlled access rights (Fig. 2b). None of the localities with fisheries restrictions had average biomass levels below 0.25  $B_0$  and 64% were above 0.5  $B_0$ , although some individual reefs within localities were below this level (Fig. 2b).

Despite extensive research into the benefits and planning of marine reserves, there is limited understanding of how long it takes reef fishes to recover once protected from fishing, limiting the ability of decision-makers to navigate management trade-offs. To estimate recovery times for fished and restricted reefs under hypothetical protection from fishing, we used the empirical recovery curve from marine reserves to back-calculate posterior virtual reserve ages ( $VA_i$ ) for each locality, given their estimated level of fish biomass. We estimated the expected age of reserves at 90% recovery ( $AR_{0.9}$ ) and subtracted the virtual reserve ages to calculate reef-specific expected recovery times ( $TR_{0.9,i}$ ) under full closure (that is,  $TR_{0.9,i} = AR_{0.9} - VA_i$ ). By sampling these quantities from the posteriors

<sup>1</sup>Australian Institute of Marine Science, PMB 3 Townsville MC, Townsville, Queensland 4810, Australia. <sup>2</sup>Department of Mathematics and Statistics, Dalhousie University, Halifax, Nova Scotia B3H 3J5, Canada. <sup>3</sup>Australian Research Council Centre of Excellence for Coral Reef Studies, James Cook University, Townsville, Queensland 4811, Australia. <sup>4</sup>Department of Parks and Wildlife, Kensington, Perth, Western Australia 6151, Australia. <sup>5</sup>Oceans Institute, University of Western Australia, Crawley, Western Australia 6009, Australia. <sup>6</sup>Coral Reef Ecosystems Division, NOAA Pacific Islands Fisheries Science Center, Honolulu, Hawaii 96818, USA. <sup>7</sup>Australian Research Council Centre of Excellence for Environmental Decisions (CEED), University of Queensland, Brisbane, St Lucia, Queensland 4074, Australia. <sup>8</sup>Wildlife Conservation Society, Marine Programs, Bronx, New York 10460, USA. <sup>9</sup>School of Marine Science and Technology, Newcastle University, Newcastle upon Tyne NE1 7RU, UK. <sup>10</sup>Fisheries Ecology Research Lab, Department of Biology, University of Hawaii, Honolulu, Hawaii 96822, USA. <sup>11</sup>Pristine Seas-National Geographic, Washington DC 20036, USA.

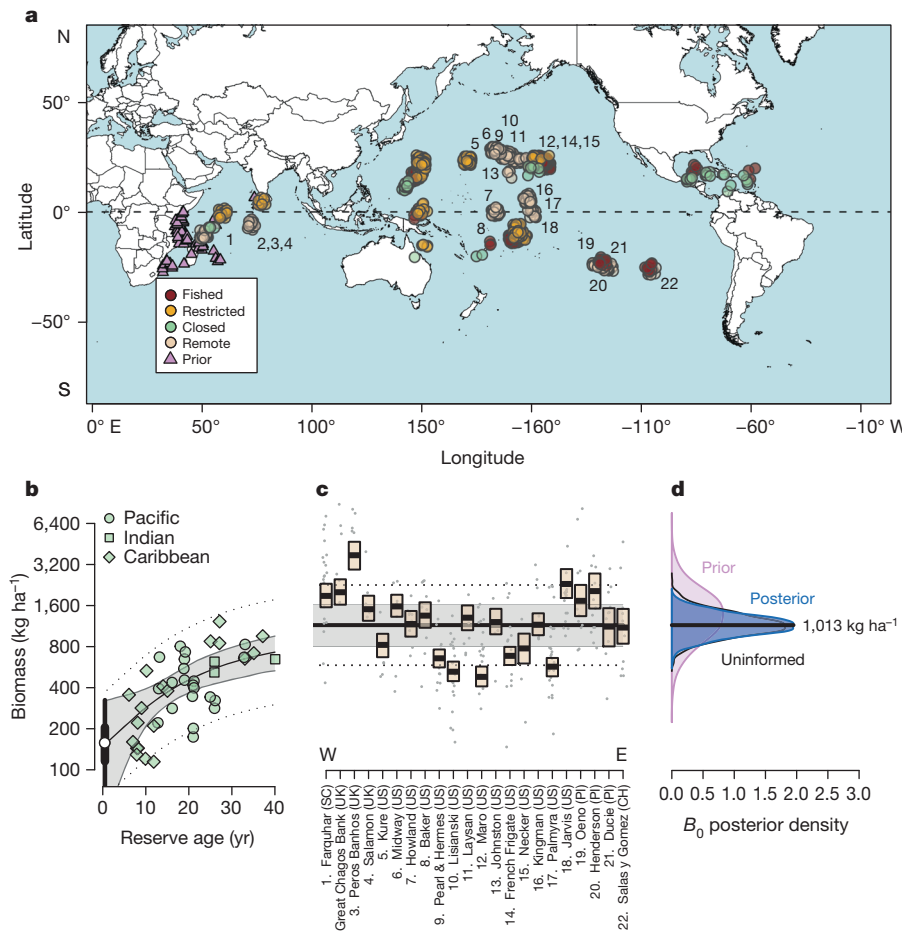


**Figure 1 | Global reef fish biomass among management categories.** **a**, Study ( $n = 832$ ) and prior ( $n = 157$ ) sites, with numbers matching graph in **c**. **b**, Posterior median recovery trajectory (black line) of reef fish biomass among reserve locations ( $n = 45$ ), with 95% uncertainty intervals (grey), 95% prediction intervals (dotted line), estimated initial biomass (white circle with 50% (thick line) and 95% (thin line) highest posterior densities), and observed

underwater visual census (UVC) data (green symbols). **c**, Posterior biomass for remote locations ( $n = 22$ ; boxplots; 50% quantiles) with data (grey circles), median  $B_0$  (black line), 95% uncertainty intervals (grey shading), and 95% prediction intervals (dotted line) from  $B_0$  in **d**. **d**, Prior (violet), joint informed (dark blue), and uninformed (black) posterior densities for  $B_0$ .

of our Bayesian model, we were able to develop probabilistic time frames for management along an expected path to recovery. Consistent with other studies on recovery benchmarks<sup>9</sup>, and the United Nations Food and Agricultural Organization (FAO) definition of underexploited fisheries being between 0.8 and 1.0 (ref. 10), we defined recovered at 0.9 of  $B_0$ , but also estimated median recovery timeframes for a range of other recovery benchmarks and rates of increase (Methods).

On average, the fished and fishing-restricted reefs surveyed within localities would require 35 years of protection from fishing to recover to 0.9  $B_0$ , while the most depleted reefs would require 59 years (Fig. 2c and Extended Data Fig. 4). Recovery times depended critically on the estimated rate of biomass recovery and the recovery benchmark used (Extended Data Fig. 5a). Although the influence of marine reserves can be detected within several years<sup>11</sup>, our global analysis supports previous case studies<sup>12,13</sup> and a meta-analysis<sup>14</sup> showing comprehensive recovery of reef fish biomass probably takes decades to achieve. This suggests that most marine reserves, having been implemented in the past 10–20 years, will require many more years to achieve their recovery potential, underscoring the need for continued, effective protection and consideration of other viable management options.

To understand how the ecosystem functions provided by fishes change with protection from fishing, we examined relative changes in functional group biomass along the gradient from collapsed ( $101 (68, 144)$  kg ha<sup>-1</sup>) to recovered ( $908 (614, 1,293)$  kg ha<sup>-1</sup>), using generalized additive models to characterize trends. Despite substantial variability in the proportion of

each functional group among reefs, clear nonlinear trends were present in relative function (Extended Data Fig. 6). During initial recovery, functional returns of key low trophic level species increased rapidly, including browsers, scraper/excavators, grazers and planktivores (Fig. 2d and Extended Data Fig. 7). These are some of the most important ecosystem functions on coral reefs, as browsers and scraper/excavators promote coral dominance by controlling algae and clearing reef substrate for coral settlement and growth<sup>15</sup>; grazers help to limit the establishment of macroalgae by intense feeding on algal turfs<sup>16</sup>; and planktivores capture water-borne nutrients and sequester them to the reef food web<sup>17</sup>. Crucially, the relative functions of grazers and scrapers/excavators reached 80–100% of their maximum biomass by 0.5  $B_0$ , while browsers, planktivores and the three top predator groups (macro-invertivores, pisci-invertivores and piscivores) increased steadily as standing biomass increased towards  $B_0$ . This overall pattern of functional change shows that key herbivore functions can be fulfilled at intermediate biomass levels, rather than solely among pristine areas.

Studies across gradients of human population and fishing densities have previously found the highest absolute losses of herbivores<sup>5</sup> and predators<sup>18,19</sup> can occur with relatively low fishing pressure; by contrast, our results show that the greatest functional changes occur when more than half of total biomass has been removed, supporting previous nonlinear relationships between biomass and function<sup>4,16</sup>. This disparity probably reflects differences in studying the effects of fishing on pristine versus altered reefs—where the apex predators not included in our analysis are readily

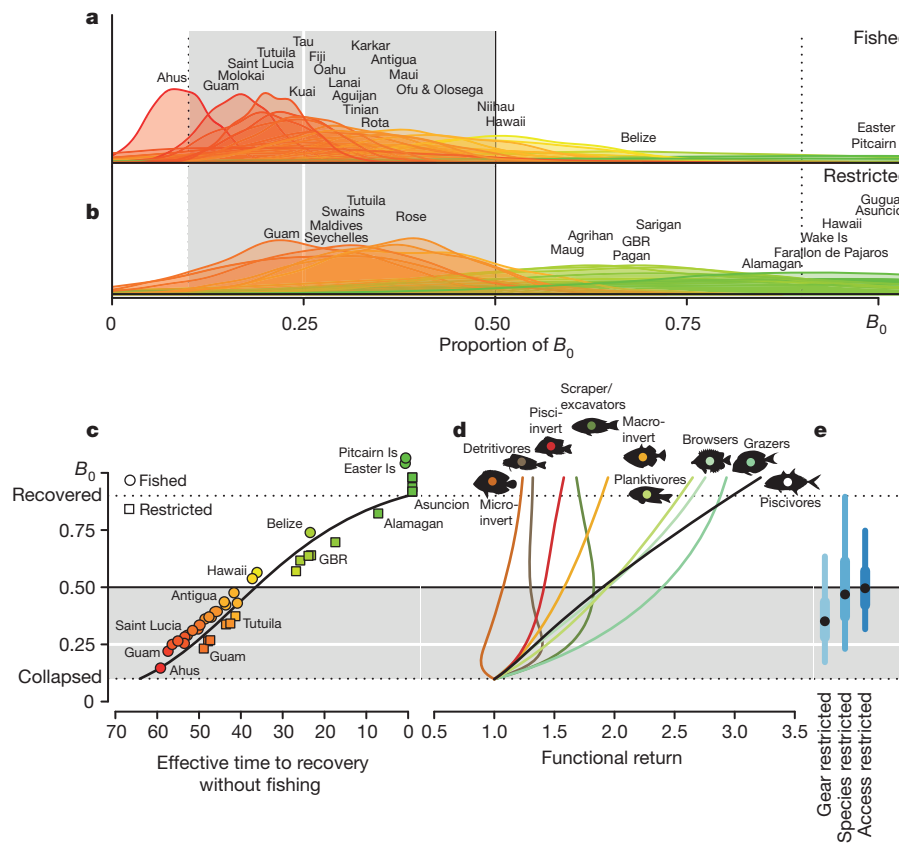


**Figure 2 | Coral reef fish responses across the spectrum of potential recovery.** **a, b**, Posterior density proportion of  $B_0$  for fished ( $n = 23$ ) (**a**) and fishing-restricted ( $n = 17$ ) (**b**) coral reef locations, shaded from red (collapsed =  $0.1 B_0$ ) to green (recovered =  $0.9 B_0$ ). GBR, Great Britain; Is., islands. **c**, Expected times to recovery ( $0.9 B_0$ ) for fished (circles) and restricted

(squares) reefs given full, effective closure. **d**, Average reef fish functional returns from collapsed to recovered. **e**, Median estimated proportion of  $B_0$  among reef fishery management alternatives (black circles) with 50% (thick line) and 95% (thin line) uncertainty intervals.

removed<sup>20</sup>—and differences in socioeconomic conditions that influence reef exploitation at specific locations<sup>21</sup>.

Although marine reserves have been widely advocated conservation tools<sup>4</sup>, they can be untenable where people depend heavily on reef-based resources, highlighting the need for management alternatives to regulate fisheries on reefs. Therefore, to complement the use of effective marine reserves, we estimated expected biomass given alternative fishing restrictions (Fig. 2e), which typically receive less resistance from fishers than marine reserves<sup>22</sup>. On average, reefs with some form of fisheries restriction had biomass 27% higher than reefs open to fishing (Fig. 2a,b). Crucially, on reefs with bans on specific fishing gears, such as beach seines, or restrictions on the types of fish that can be caught, such as herbivores, biomass levels were between 0.3 and 0.4  $B_0$ , the point at which up to 80% of herbivore function was retained (Fig. 2e). Thus, even simple fisheries restrictions can have substantial effects on fish functional groups that support important reef processes. Still greater biomass and functional returns were observed on reefs with access restrictions limiting the number of people allowed to fish a reef, such as family relations, or where other forms of established local marine tenure enable exclusion of external fishers<sup>21</sup>. Although these management alternatives clearly promote important functional gains relative to openly fished reefs, it is only among well-enforced, long-established marine reserves that predation is maximized, more than tripling the function of piscivory present on collapsed reefs.

The continuing degradation of the world's coral reefs underscores the need for tangible solutions that promote recovery and enhance ecosystem functions<sup>4,23</sup>. Our results demonstrate that well-enforced marine reserves can support a full suite of reef fish functions given enough time to recover. However, for reefs where marine reserves cannot be implemented, we find that ecosystem functions can be enhanced through various forms

of fisheries management. Addressing the coral reef crisis ultimately demands long-term, international action on global-scale issues such as ocean warming and acidification<sup>24</sup>, factors that may diminish recovery potential by ~6% over the coming decades (Extended Data Fig. 5b). Despite these challenges, a range of fisheries management options is available to support reef resilience and it is likely that some combination of approaches will be necessary for success. Having benchmarks and timelines within an explicit biomass context, such as those provided here, increase the chances of agreeing on, and complying with, a mix of management strategies that will achieve conservation objectives while sustaining reef-based livelihoods.

**Online Content** Methods, along with any additional Extended Data display items and Source Data, are available in the online version of the paper; references unique to these sections appear only in the online paper.

Received 4 July 2014; accepted 27 February 2015.

Published online 8 April 2015.

- Hughes, T. P. et al. Rising to the challenge of sustaining coral reef resilience. *Trends Ecol. Evol.* **25**, 633–642 (2010).
- Graham, N. A. J. et al. Managing resilience to reverse phase shifts in coral reefs. *Front. Ecol. Environ.* **11**, 541–548 (2013).
- Dulvy, N. K., Freckleton, R. P. & Polunin, N. V. C. Coral reef cascades and the indirect effects of predator removal by exploitation. *Ecol. Lett.* **7**, 410–416 (2004).
- McClanahan, T. R. et al. Critical thresholds and tangible targets for ecosystem-based management of coral reefs. *Proc. Natl Acad. Sci. USA* **108**, 17230–17233 (2011).
- Bellwood, D. R. et al. Human activity selectively impacts the ecosystem roles of parrotfishes on coral reefs. *Proc. R. Soc. Lond. B* **279**, 1621–1629 (2012).
- Edgar, G. J. et al. Global conservation outcomes depend on marine protected areas with five key features. *Nature* **506**, 216–220 (2014).

7. Newton, K. *et al.* Current and future sustainability of island coral reef fisheries. *Curr. Biol.* **17**, 655–658 (2007).
8. Worm, B. *et al.* Rebuilding global fisheries. *Science* **325**, 578–585 (2009).
9. Lambert, G. I. *et al.* Quantifying recovery rates and resilience of seabed habitats impacted by bottom fishing. *J. Appl. Ecol.* **51**, 1326–1336 (2014).
10. Worm, B. & Branch, T. A. The future of fish. *Trends Ecol. Evol.* **27**, 594–599 (2012).
11. Babcock, R. C. *et al.* Decadal trends in marine reserves reveal differential rates of change in direct and indirect effects. *Proc. Natl Acad. Sci. USA* **107**, 18256–18261 (2010).
12. McClanahan, T. R., Graham, N. A. J., Calnan, J. & MacNeil, M. A. Towards pristine biomass: reef fish recovery in coral reef marine protected areas in Kenya. *Ecol. Appl.* **17**, 1055–1067 (2007).
13. Russ, G. R. & Alcala, A. C. Decadal-scale rebuilding of predator biomass in Philippine marine reserves. *Oecologia* **163**, 1103–1106 (2010).
14. Molloy, P. P., McLean, I. B. & Côté, M. Effects of marine reserve age on fish populations: a global meta-analysis. *J. Anim. Ecol.* **46**, 743–751 (2009).
15. Rasher, D. B. *et al.* Consumer diversity interacts with prey defenses to drive ecosystem function. *Ecology* **94**, 1347–1358 (2013).
16. Mumby, P. J. *et al.* Empirical relationships among resilience indicators on Micronesian reefs. *Coral Reefs* **32**, 213–226 (2013).
17. Hamner, W. H. *et al.* Export-import dynamics of zooplankton on a coral reef in Palau. *Mar. Ecol. Prog. Ser.* **334**, 83–92 (2007).
18. Jennings, S. *et al.* Effects of fishing effort and catch rate upon the structure and biomass of Fijian reef fish communities. *J. Appl. Ecol.* **33**, 400–412 (1996).
19. Dulvy, N. K. *et al.* Size structural change in lightly exploited coral reef fish communities: evidence for weak indirect effects. *Can. J. Fish. Aquat. Sci.* **61**, 466–475 (2004).
20. Robbins, W. D., Hisano, M., Connolly, S. R. & Choat, J. H. Ongoing collapse of coral-reef shark populations. *Curr. Biol.* **16**, 2314–2319 (2006).
21. Cinner, J. E. *et al.* Co-management of coral reef social-ecological systems. *Proc. Natl Acad. Sci. USA* **109**, 5219–5222 (2012).
22. McClanahan, T. R., Abunge, C. A. & Cinner, J. E. Heterogeneity in fishers' and managers' preferences towards management restrictions and benefits in Kenya. *Environ. Conserv.* **39**, 357–369 (2012).
23. Bellwood, D. R., Hughes, T. P., Folke, C. & Nyström, M. Confronting the coral reef crisis. *Nature* **429**, 827–833 (2004).
24. Hoegh-Guldberg, O. *et al.* Coral reefs under rapid climate change and ocean acidification. *Science* **318**, 1737–1742 (2007).

**Supplementary Information** is available in the online version of the paper.

**Acknowledgements** We thank M. Emslie, A. Cheal, J. Wetherall, C. Hutchery and K. Anthony for comments on early drafts of the manuscript. The Australian Institute of Marine Science, the ARC Centre of Excellence for Coral Reef Studies, and the John D. and Catherine T. MacArthur Foundation supported this research.

**Author Contributions** M.A.M. conceived of the study with N.A.J.G., N.V.C.P., T.R.M., S.K.W. and J.E.C.; M.A.M. developed and implemented the analysis; M.A.M. led the manuscript with N.A.J.G., J.E.C. and S.K.W. All other authors contributed data and made substantive contributions to the text.

**Author Information** This is Social Ecological Research Frontiers (SERF) working group contribution number 10. Reprints and permissions information is available at [www.nature.com/reprints](http://www.nature.com/reprints). The authors declare no competing financial interests. Readers are welcome to comment on the online version of the paper. Correspondence and requests for materials should be addressed to M.A.M. ([a.macneil@aims.gov.au](mailto:a.macneil@aims.gov.au)).

## METHODS

Reef fish biomass estimates were based on instantaneous visual counts (UVC) from 2,096 surveys collected from coral reef slopes (that is, the sloping, windward outer reef, selected specifically to standardize the reef habitat and remove potential bias associated with habitat type) on 832 individual reef sites (hereafter 'reef'). No statistical methods were used to predetermine sample size. All data were collected using standard belt transects ( $50 \times 5$  m or  $30 \times 4$  m) or point-counts (7 m radius) between 2002 and 2013, with the bulk of the data (92%) collected since 2006 (Supplementary Table 1). Data from belt transects and point counts have repeatedly been shown to be comparable in estimating fish abundance<sup>25</sup> and biomass<sup>26</sup>. Within each survey area, reef associated fishes were identified to species level, abundance counted, and total length estimated to the nearest 5 cm. A single experienced observer collected data for each data set except the NOAA data from the Pacific where multiple observers operate on every sampling mission. However, NOAA has extensive protocols in place to ensure that their observers are well trained and follow consistent protocols, ensuring the data are consistent and unbiased. We tested for any bias among data providers (capturing information on both inter-observer differences, and census methods) by including each data provider as a random effect in our model (see below), which assumes that there are inherent correlations within data sets that affect the means and associated errors estimated from their data. This analysis showed that there was no bias among data providers and that there is little information present in data provider identities (Extended Data Fig. 2). From these transect-level data, we retained counts of diurnally active, non-cryptic reef fish that are resident on the reef slope, excluding sharks and semi-pelagics (Supplementary Table 2). Metadata for the surveys are within the James Cook University research data repository, the Tropical Data Hub (<https://ereresearch.jcu.edu.au/tdh>).

Total biomass of fishes on each transect was calculated using published length-weight relationships or those available on FishBase (<http://fishbase.org>). During this process, we removed 35 transects in which divers were mobbed by behaviourally aggregating species (for example, *Acanthurus coeruleus*;  $n = 34$ ) or high biomass aggregating species (*Bolbometopon muricatum*;  $n = 1$ ) that led to potentially unreliable estimates of standing biomass according to the data provider. This truncated data set was averaged to the reef level (that is, transects within the same section of continuous reef)<sup>27</sup> forming 832 distinct reefs that formed the basic data for our study. The data were sampled from key coral regions around the world; however, the coral triangle, Brazil, West Africa and the Red Sea/Arabian Sea regions are not represented. Fish species were assigned to functional groups based on trophic guilds and dietary information from the literature and FishBase. A key scale in our analysis was 'locality', defined as reef areas from 10s to 100s of kilometres that generally correspond to individual nations and map closely onto ranges of human influence<sup>27</sup>, within which reefs were nested for analysis. In this way our analysis consisted of three spatial scales: reef, locality and global.

We used the PyMC package<sup>28</sup> for the Python programming language to conduct our analysis, running the (Metropolis–Hastings) MCMC sampler for  $10^6$  iterations, with a 900,000 iteration burn in and a thinning rate of 100, leaving 1,000 samples in the posterior of each parameter; these long (relative to Gibbs sampling, for example) burn-in times are often required with a Metropolis–Hastings algorithm. Convergence was monitored by examining posterior chains and distributions for stability and by running five chains from different starting points and checking for convergence using Gelman–Rubin statistics<sup>29</sup> for parameters across multiple chains, all of which were at or close to 1, indicating good convergence of parameters across multiple chains.

We used multiple data sources, including remote areas, asymptotes of well enforced marine reserves, and prior information, to estimate unfished biomass ( $B_0$ ) and time for recovery. Remote areas, defined as having no recent history of fishing and being more than 200 km from human settlement, informed local  $B_{0l}$  and global  $B_0$ , given reef-specific covariates  $x_{nj}$  thought to influence standing biomass that were available at most localities. These covariates included local net primary production (NPP)<sup>30</sup>, average proportion of hard coral cover<sup>31</sup>, depth of survey (m)<sup>32</sup>, and having been collected on an atoll (0/1 dummy variable)<sup>33</sup>. NPP was calculated as ensemble mean of estimates based on two NPP algorithms applied on MODIS and SeaWiFS data (that is, Carbon-based Production Model-2 (CbPM2)<sup>34</sup> and Vertically Generalized Production Model (VGPM; <http://orca.science.oregonstate.edu>)<sup>35</sup>; mg C m<sup>-2</sup> day<sup>-1</sup>). Each of these reef-specific nuisance parameters were mean centred to offset the reef level observations relative to the main focus of our model—the  $B_{0l}$  estimates.

To ensure an appropriate sub-model structure was used, we evaluated fits of three potential linear and nonlinear relationships (linear, second-order polynomial, and third-order polynomial) for each continuous nuisance parameter. We selected the best-fitting relationship for each nuisance parameter individually based on having the lowest deviance information criteria (DIC) value (Extended Data Table 1) and then compared DIC values of a candidate model set having all combinations of each nuisance parameter to select a final model (Extended Data Table 2). We also examined the posterior residuals for each nuisance parameter sub-model to ensure no heteroscedasticity was present and that errors were normally distributed (Extended Data Fig. 8).

To recognize potential data provider methodological effects, we incorporated data-provider status in our  $B_0$  estimates by adding a random effect  $\rho_j$  for data provider  $j$  in our Bayesian hierarchical model. These factors were included in a log-normal hierarchical model for  $B_0$ , given reef-scale observations  $y_{il,r}$ :

$$y_{il,r} \sim N(\mu_{il,r}, \sigma_l) \quad (1)$$

$$\begin{aligned} \mu_{il,r} = B_{0l} + \beta_1 x_{coral,i} + \beta_2 x_{coral,i}^2 + \beta_3 x_{coral,i}^3 + \beta_4 x_{atoll,i} + \beta_5 x_{production,i} \\ + \beta_6 x_{production,i}^2 + \beta_7 x_{production,i}^3 + \rho_j \end{aligned} \quad (2)$$

$$B_{0l} \sim N(B_0, \sigma_b), \quad (3)$$

and weakly-informative priors

$$\beta_{1,\dots,7} \sim N(0, 0.100) \quad (4)$$

$$\sigma_{l,b} \sim U(0.0, 100) \quad (5)$$

$$\rho_j \sim N(0.0, 100). \quad (6)$$

Because this study built on previous research conducted in the western Indian Ocean<sup>7</sup> we used the posterior  $B_0$  estimate from that study as the prior for our analysis:

$$B_0 \sim LN(7.08, 0.46) \quad (7)$$

allowing us to build on existing knowledge by directly integrating information between studies. As a check for those averse to building on previous research in this way, we also ran the full model using an uninformative  $B_0$  prior, resulting in highly similar inferences, albeit with marginally greater uncertainty than the informed estimates ( $6.92$  ( $6.52, 7.27$ )  $\log(\text{kg ha}^{-1})$  informed;  $6.82$  ( $6.45, 7.23$ )  $\log(\text{kg ha}^{-1})$  uninformative), demonstrating that the observed data dominated the prior in our analysis.

To estimate times to biomass recovery, we relied on data from well-enforced, previously fished marine reserves from around the world (Fig. 1a) and used a space-for-time substitution approach, assuming the relationship between reserve age and standing biomass follows a standard logistic regression model and the same reef-scale offset terms as above:

$$y_{i,a} \sim N(\mu_a, \sigma_m) \quad (8)$$

$$\begin{aligned} \mu_a = \frac{B_0}{1 + (B_0 - \mu_0)/\mu_0} e^{-ra} + \beta_1 x_{coral,i} + \beta_2 x_{coral,i}^2 + \beta_3 x_{coral,i}^3 + \beta_4 x_{atoll,i} \\ + \beta_5 x_{production,i} + \beta_6 x_{production,i}^2 + \beta_7 x_{production,i}^3 + \rho_j \end{aligned} \quad (9)$$

Here  $a$  is the age of the marine reserve in years;  $\mu_0$  is the average initial reserve biomass; and  $r$  the average rate of biomass increase. This model is less hierarchically explicit than equation (2) owing to the scarcity of global marine reserve biomass data, and relies on the key assumption that average reserve potential recovery is consistent, absent the reef-scale effects in the model. Notably,  $B_0$  is the same as in equation (3) and the linear offsets  $\beta_{1,\dots,7}$  the same as in (2), meaning their effects were jointly estimated from both remote and marine reserve data. Therefore,  $B_0$  is estimated from both the trajectory of marine reserves through time and from the average biomass of all areas defined a priori as being remote:  $B_0$  is the asymptote in the reserve component of the model and the global mean in the remote component of the model.  $\mu_0$ , the minimum biomass at reserve age zero, was given an uninformative  $\sim U(1, 10)$  prior that spanned the range of the data; the standard deviation  $\sigma_m$  was as in (5);  $x_{size,i}$  was set to allow for potential effects of reserve size, thought to be an important component of reserve success<sup>6</sup>.

Next we estimated standing reef fish biomass across a range of fished locations, again hierarchically, given observer effects and reef-level observations within each location:

$$y_{il,f} \sim N(\mu_{il,f}, \sigma_f) \quad (10)$$

$$\begin{aligned} \mu_{il,f} = B_{lf} + \beta_1 x_{coral,i} + \beta_2 x_{coral,i}^2 + \beta_3 x_{coral,i}^3 + \beta_4 x_{atoll,i} + \beta_5 x_{production,i} \\ + \beta_6 x_{production,i}^2 + \beta_7 x_{production,i}^3 + \rho_j \end{aligned} \quad (11)$$

$$B_{lf} \sim N(0.0, 100) \quad (12)$$

Here the  $B_{lf}$  terms denote independent log-biomass priors per location as we did not assume any parent (hierarchical) structure among locations other than potential data-provider effects; the standard deviation prior for  $\sigma_f$  was as in (5). Note that fishing pressure is a continuous variable that implicitly underlies the observed differences in exploitation state outside of the factors included in our analysis.

To estimate the standing biomass across a range of management categories,  $z$ , we applied similar methods:

$$y_{il,z} \sim N(\mu_{il,z}, \sigma_z) \quad (13)$$

$$\begin{aligned} \mu_{il,z} = & B_{l,z} + \beta_1 x_{\text{coral},i} + \beta_2 x_{\text{coral},i}^2 + \beta_3 x_{\text{coral},i}^3 + \beta_4 x_{\text{atoll},i} + \beta_5 x_{\text{production},i} \\ & + \beta_6 x_{\text{production},i}^2 + \beta_7 x_{\text{production},i}^3 + \rho_j \end{aligned} \quad (14)$$

$$B_{l,z} \sim N(0, 0.100) \quad (15)$$

As for the fished locations, the  $B_{l,z}$  terms denote independent log-biomass priors per location and the standard deviation prior for  $\sigma_z$  was as in (5). Management alternative effects were calculated as the average of the location-level posteriors for each group. Note that some locations in the data (Agrihan, Alamagan, Asuncion, Farallon de Pajaros, Guguan, Maug, Pagan, Rose and Sarigan) were passively fishery-restricted owing to isolation limiting effort that could be directed at the resource and, as a trait that cannot be actively managed, we excluded these locations from this section of our analysis.

**Overall model fit.** We conducted posterior predictive checks for goodness of fit using Bayesian  $P$  values<sup>36</sup>, whereby fit was assessed by the discrepancy between observed or simulated data and their expected values. To do this we simulated new data ( $y_i^{\text{new}}$ ) by sampling from the joint posterior of our model ( $\theta$ ) and calculated the Freeman–Tukey measure of discrepancy for the observed ( $y_i^{\text{obs}}$ ) or simulated data, given their expected values ( $\mu_i$ ):

$$D(y|\theta) = \sum_i (\sqrt{y_i} - \sqrt{\mu_i})^2 \quad (16)$$

yielding two arrays of median discrepancies  $D(y^{\text{obs}}|\theta)$  and  $D(y^{\text{new}}|\theta)$  that were then used to calculate a Bayesian  $P$  value for our model by recording the proportion of times  $D(y^{\text{obs}}|\theta)$  was greater than  $D(y^{\text{new}}|\theta)$  (Extended Data Fig. 3). For models not showing evidence of being inconsistent with the observed data,  $D(y^{\text{obs}}|\theta)$  will be greater than  $D(y^{\text{new}}|\theta)$  50% of the time, giving  $P = 0.5$ ; for models showing evidence of being inconsistent with the observed data,  $D(y^{\text{obs}}|\theta)$  will, by specification, be greater than (or less than)  $D(y^{\text{new}}|\theta)$  95% of the time.

**Times to recovery.** We capitalized on our integrated Bayesian model to estimate location-specific recovery times for fished and fishery-restricted reefs within the Bayesian MCMC scheme. First we calculated the average reserve age at recovery (that is,  $0.9B_0$ :  $B_{0.9}$ ), given the posterior biomass rate of growth  $r$  and initial biomass of  $\mu_0$  (see posterior parameter estimates in Supplementary Table 3):

$$\text{AR}_{0.9} = \frac{\log \left[ \left( \frac{B_0}{B_{0.9}} - 1 \right) / \left( \frac{B_0 - \mu_0}{\mu_0} \right) \right]}{-r} \quad (17)$$

Next we calculated location-specific virtual reserve ages, given their estimated level of log-biomass:

$$\text{VA}_i = \frac{\log \left[ \left( \frac{B_0}{B_{i,f/z}} - 1 \right) / \left( \frac{B_0 - \mu_0}{\mu_0} \right) \right]}{-r} \quad (18)$$

and subtracted this from  $\text{AR}_{0.9}$  to give an expected time to recovery for each location:

$$\text{TR}_{0.9,i} = \text{AR}_{0.9} - \text{VA}_i \quad (19)$$

Because these calculations were conducted within our MCMC scheme they included posterior uncertainties, given the data and our model.

**Variable recovery targets.** Our choice to define recovery at  $0.9B_0$  was based on recent work on recovery in the North Sea<sup>9</sup> and being the midpoint at which individual fish stocks are considered underexploited by the United Nations Food and Agricultural Organization<sup>10</sup>. However, to explore how expected time to recovery was dependent on this choice and the estimated rate of biomass growth, we calculated average reserve ages at recovery ( $\text{AR}_{x,y}$ ) using the median posterior  $B_0$  and  $\mu_0$  values (in (17)) while systematically varying the proportion of  $B_0$  defined as recovered (between 0.8 to 1.0) and the rate of biomass growth (between posterior 95% UI range of 0.012 and 0.11). The resulting surface plot showed exponential increases in reserve ages at recovery for slower biomass growth rates and higher values of defined recovery due to the asymptotic nature of the logistic growth model used. (Extended Data Fig. 5).

**Potential effects of climate change on  $B_0$ .** A key assumption of the conclusions drawn from our results is that factors affecting total potential  $B_0$  will remain stable through time. Climate projections have been equivocal as to what might happen to tropical fisheries over the coming decades<sup>37</sup>, primarily owing to uncertainty in how production<sup>38</sup> and hard coral habitat<sup>39</sup> is expected to change, as well as difficulty in modelling tropical coastal habitats<sup>37</sup>. Nonetheless, we used the estimated relationships of log-biomass to productivity and hard coral cover (Extended Data Fig. 1) to

explore changes in  $B_0$  owing to declines in both environmental conditions, using the median posterior estimates from our Bayesian hierarchical model. Results showed that by 2040, given an expected 4% loss of primary productivity<sup>38</sup> and a 2% annual loss of coral cover<sup>39</sup>, we would expect to see a 6% drop in  $B_0$ , to 953 kg ha<sup>-1</sup> (Extended Data Fig. 5b).

**Log versus arithmetic scales of estimation.** By adopting a hierarchical approach we, in effect, chose to average over location-specific differences to make global-scale inferences. We elected to model our data on the log-scale, as per fisheries convention<sup>40</sup>, because it normalized the variance around our hierarchical model, greatly improving the precision of model estimates and the convergence of our model fits.

A key related point in our analysis is that our posterior calculations for fractions of  $B_0$  were all on the arithmetic scale, by exponentiating each location-scale estimate and dividing by  $e^{B_0}$ . To see why this makes sense, taking the posterior estimates for log-biomass from Ahus, PNG (4.54) and  $B_0$  (6.92), Ahus would have retained  $4.54/6.92 = 0.66$  unfished log-biomass but only  $e^{4.54}/e^{6.92} = 0.09$  absolute biomass. Given that this is the most heavily exploited reef in our database and that fisheries conventions for defining collapsed and recovered are arithmetic, we retained the arithmetic for our posterior calculations.

**Functional returns.** To understand how relative reef fish function would be expected to vary over the recovery range from collapsed (101 (68, 143) kg ha<sup>-1</sup>) through to recovery (908 (614, 1293) kg ha<sup>-1</sup>), we modelled the average biomass of each functional group across this range (that is,  $\log(101)$  to  $\log(908)$  kg ha<sup>-1</sup>) relative to their initial biomass values (that is, average biomass of each functional group at  $\log(101)$  kg ha<sup>-1</sup>). We deemed these relative changes in biomass ‘functional returns’ because they express relative increases in function that could be expected given log-scale increases in the total biomass of a given functional group on a coral reef. To do this, and allow for expected non-linearities in functional group responses (due to, for example, community interactions, resource dynamics, the shape of response to which is currently unknown for most functional groups) we fit a series of generalized additive models (GAMs) to the proportion of each functional group over the community recovery range (Extended Data Fig. 6) in models that included the same covariates as our Bayesian hierarchical model (NPP, average proportion of hard coral cover, depth of survey, and having been collected on an atoll). The form of the model was, for each functional group  $k$ :

$$y_{il,k} \sim N(\mu_{il,k}, \sigma_k) \quad (20)$$

$$\mu_{il,k} = \beta_{0l} + f_1(x_{\log-\text{biomass},i}) + \beta_1 x_{\text{coral},i} + \beta_2 x_{\text{atoll},i} + \beta_3 x_{\text{production},i} \quad (21)$$

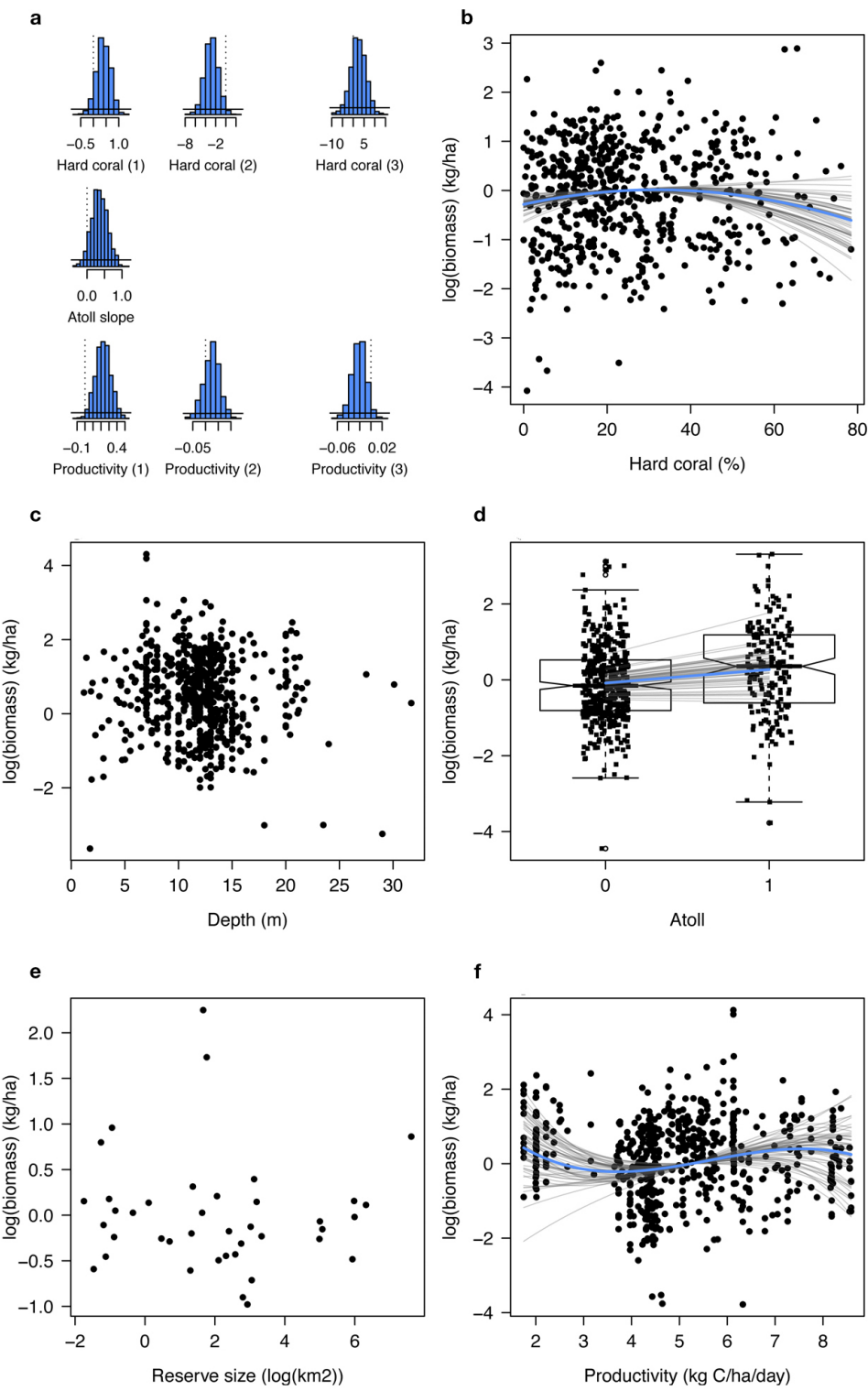
$$\beta_{0l} \sim N(0, 0.100). \quad (22)$$

with the smooth function  $f_1(x_{\log-\text{biomass},i})$  describing the nonlinear relationship between observed functional group proportions and total log-biomass. Dividing the fitted GAMs for each functional group by the proportion at collapse provided a measure of expected functional return for each group, where a functional return of 2.0 would mean there is twice the log-biomass of a given functional group present compared to initial conditions. The rationale for this approach was that, as our data span the full range from 0.1 to 0.9  $B_0$ , we did not need to predict outside of the data, but rather uncover the potentially nonlinear changes in relative function for each group over this range. All GAMs were run using in the GAMM package in R (<http://www.r-project.org>), using default smooth parameters that provided consistent fits to a per 0.1 log-kg moving average.

**Code availability.** The data set used in this analysis can be obtained from the corresponding author on request, and combined with PyMC code in the Supplementary Methods to replicate our Bayesian hierarchical analysis.

25. Samoilys, M. A. & Carlos, G. Determining methods of underwater visual census for estimating the abundance of coral reef fishes. *Environ. Biol. Fishes* **57**, 289–304 (2000).
26. Watson, R. A. & Quinn, T. J. Performance of transect and point count underwater visual census methods. *Ecol. Model.* **104**, 103–112 (1997).
27. MacNeil, M. A. & Connolly, S. R. In *Ecology of Fishes on Coral Reefs: The Functioning of an Ecosystem in a Changing World* Ch. 12 (ed. Mora, C.) (Cambridge Univ. Press, 2015).
28. Patil, A., Huard, D. & Fonnesbeck, C. J. PyMC: Bayesian stochastic modelling in Python. *J. Stat. Softw.* **35**, 1–81 (2010).
29. Gelman, A. & Rubin, D. B. Inference from iterative simulation using multiple sequences. *Stat. Sci.* **7**, 457–472 (1992).
30. Chassot, E. et al. Global marine primary production constrains fisheries catches. *Ecol. Lett.* **13**, 495–505 (2010).
31. Graham, N. A. J. et al. Climate warming, marine protected areas and the ocean-scale integrity of coral reef ecosystems. *PLoS ONE* **3**, e3039 (2008).
32. Newman, M. J. H., Paredes, G. A., Sala, E. & Jackson, J. B. C. Structure of Caribbean coral reef communities across a large gradient of fish biomass. *Ecol. Lett.* **9**, 1216–1227 (2006).

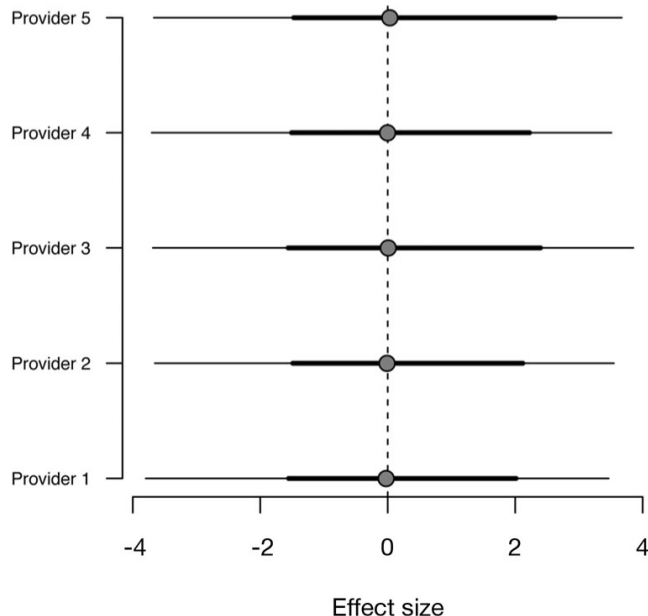
33. Cinner, J. E., Graham, N. A. J., Huchery, C. & MacNeil, M. A. Global effects of local human population density and distance to markets on the condition of coral reef fisheries. *Conserv. Biol.* **27**, 453–458 (2013).
34. Westberry, T., Bherenfeld, M. J., Siegel, D. A. & Boss, E. Carbon-based primary productivity modeling with vertically resolved photoacclimation. *Global Biogeochem. Cy.* **22**, GB2024 (2008).
35. Behrenfeld, M. J. & Falkowski, P. G. Photosynthetic rates derived from satellite-based chlorophyll concentration. *Limnol. Oceanogr.* **42**, 1–20 (1997).
36. Brooks, S. P., Catchpole, E. A. & Morgan, B. J. T. Bayesian animal survival estimation. *Stat. Sci.* **15**, 357–376 (2000).
37. Cheung, W. W. L. et al. Large-scale redistribution of maximum fisheries potential in the global ocean under climate change. *Glob. Change Biol.* **16**, 24–35 (2010).
38. Sarmiento, J. L. et al. Response of ocean ecosystems to climate warming. *Glob. Biogeochem. Cycles* **18**, GB3003 (2004).
39. Bruno, J. F. & Selig, E. R. Regional decline of coral cover in the indo-pacific: timing, extent, and subregional comparisons. *PLoS ONE* **3**, e711 (2007).
40. Walters, C. J. & Martell, S. J. D. *Fisheries Ecology and Management* (Princeton Univ. Press, 2004).



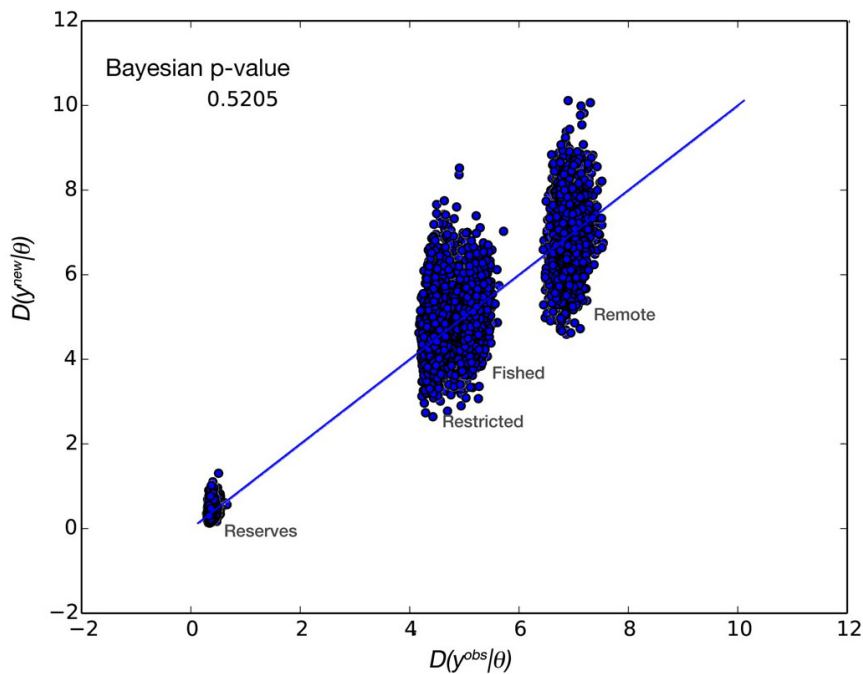
**Extended Data Figure 1 | Nuisance parameter posterior estimates for modelled recovery.** **a**, Joint Bayesian hierarchical recovery model. Prior (flat black line) and posterior (histograms) nuisance parameter densities (vertical dotted line at zero) for factors influencing total reef fish biomass ( $\text{kg ha}^{-1}$ ), including three parameters for a third order polynomial for hard coral cover (that is, hard coral (1), (2), (3)), an offset for atoll versus non-atoll, and three parameters for a third order polynomial for productivity (that is, productivity (1), (2), (3)). **b**, Estimated relationship between percentage hard coral cover and total biomass using posterior median values (blue line), with 99 samples

from the posterior distribution of the parameters in **a** (thick grey lines) and marginal data (black dots;  $n = 832$  reefs).

**c**, Plot of observed depth and marginal total biomass given the full model (no depth effect present). **d**, Estimated relationship between atoll (1) versus non-atoll (0) and total biomass, with marginal data (boxplot and black squares). **e**, Plot of reserve size and marginal total fish biomass given the full model (no reserve size effect present). **f**, Estimated relationship between productivity and total biomass, with marginal data.

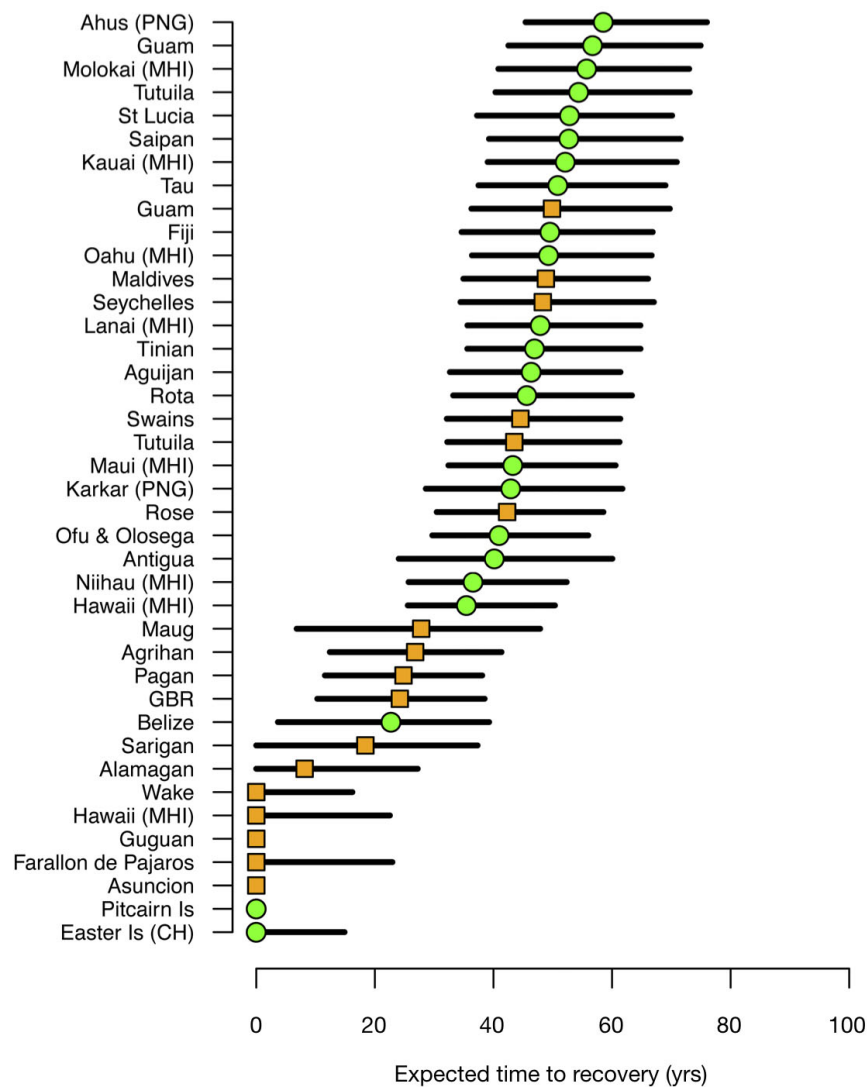


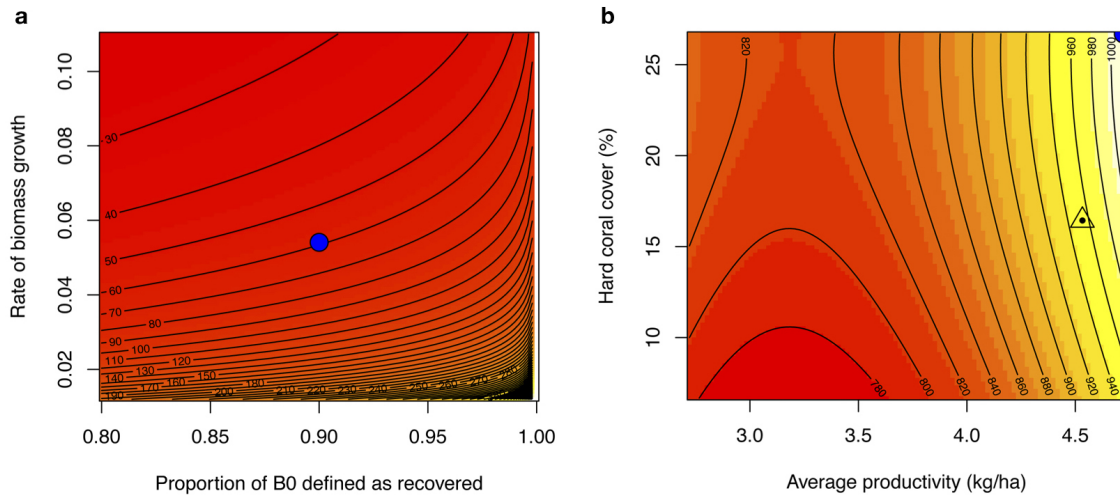
**Extended Data Figure 2 | Data provider random effect posteriors.** Bayesian hierarchical model posterior estimated effects of data provider identity, including 95% posterior densities (thin lines), 50% posterior densities (thick lines), and posterior median values (black circles). Results show no apparent bias among data providers, with little information present in provider identities.

**Extended Data Figure 3 | Bayesian  $P$  values for goodness of fit.**

Discrepancy-based posterior predictive checks for Bayesian hierarchical model goodness of fit. Points represent Freeman–Tukey discrepancy measures between observed and expected values,  $D(y^{\text{obs}}|\theta)$ , and simulated and expected

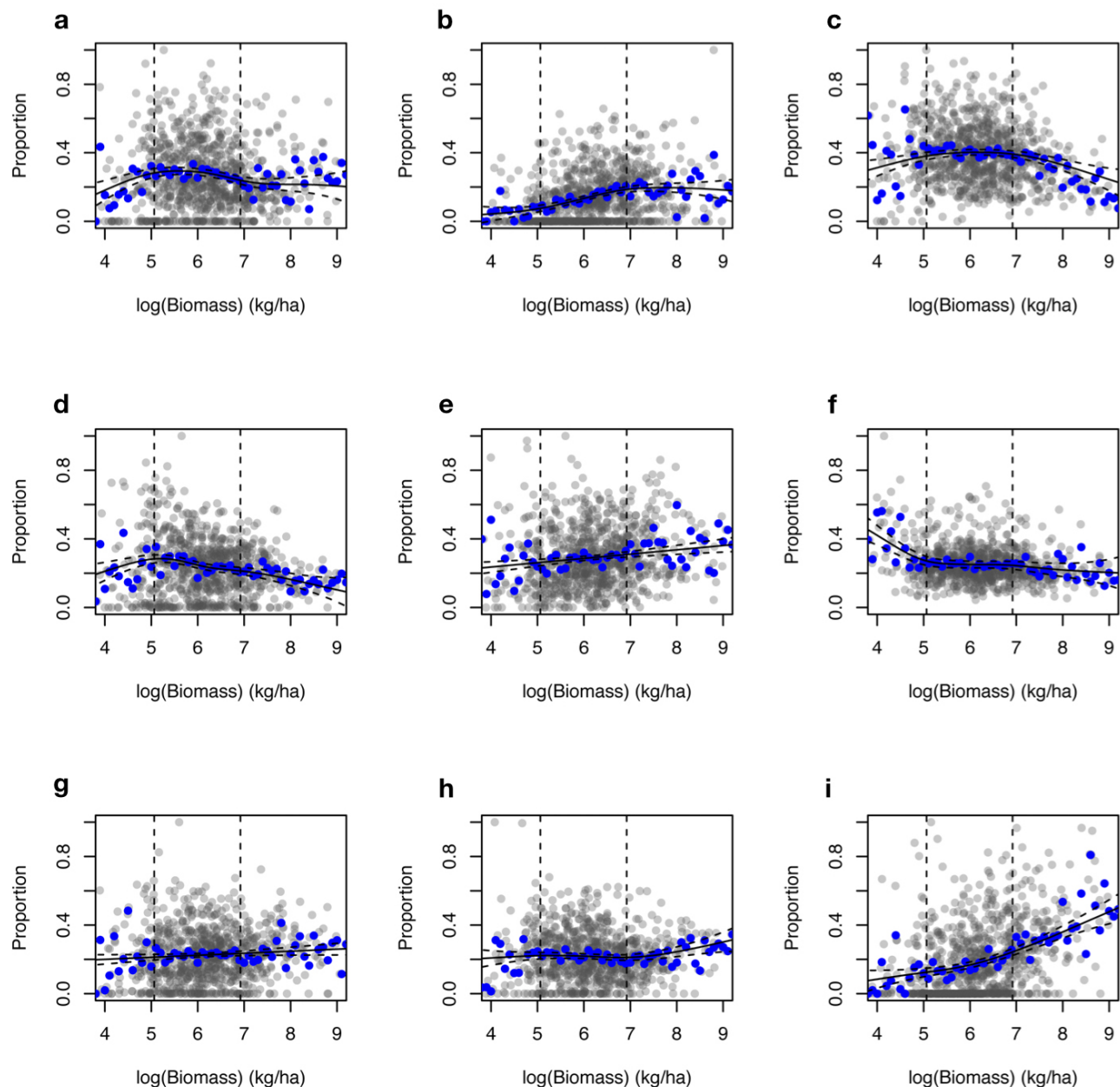
values,  $D(y^{\text{new}}|\theta)$ . Plot shows high level of agreement between observed and simulated discrepancies ( $P = 0.521$ ), indicating the model is not inconsistent with the observed data. Labelled clusters of distinct points reflect various components of the joint model.





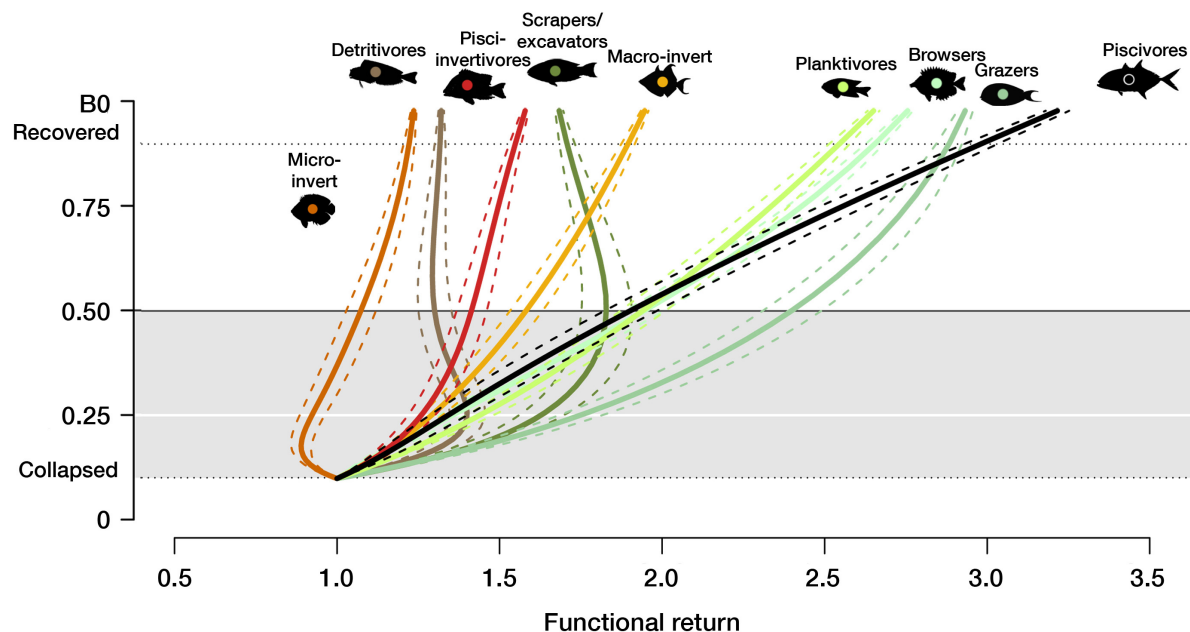
**Extended Data Figure 5 | Change in expected reserve age and potential effects under climate change.** **a**, Change in expected reserve age at recovery (contour lines; in years) given specified values for recovery (as a proportion of  $B_0$ ) and the 95% highest posterior density range for the rate of biomass growth ( $r_0$ ) estimated from a joint Bayesian hierarchical model of recovery. Expected recovery time from the most degraded locality (Ahus, PNG; posterior median:  $94 \text{ kg ha}^{-1}$ ) given  $r_0$  (posterior median: 0.054) is 59 years when recovery is defined at 0.9  $B_0$  (blue dot). **b**, Response surface (contour lines) for potential

change in  $B_0$  ( $\text{kg ha}^{-1}$ ) given a plausible range of decline in average primary productivity (from current  $4.7 \text{ kg C ha}^{-1} \text{ day}^{-1}$ ) and coral cover (from current 26% average hard coral cover). Response surface based on model estimated effects of productivity and hard coral cover on  $B_0$  (Extended Data Fig. 1). Current conditions are in the top right (blue dot); a plausible scenario for 2040 given a 4% loss of primary productivity and a 2% annual loss of coral cover would lead to a 6% drop in expected  $B_0$ , down to  $953 \text{ kg ha}^{-1}$  (dot-triangle).



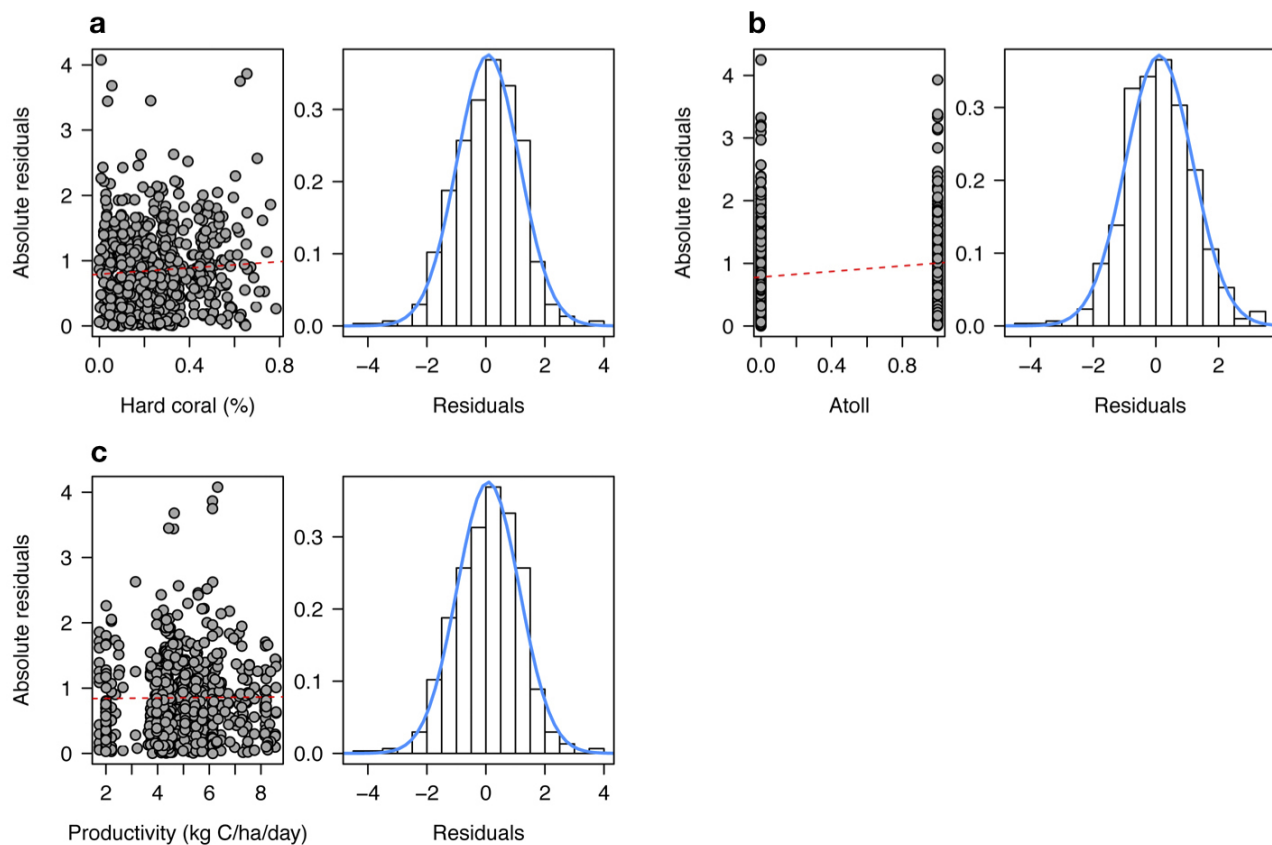
**Extended Data Figure 6 | Average reef fish functional group across a biomass gradient.** **a–i**, Generalized additive model (GAM) fits to the relative proportion of excavators/scrapers (**a**), browsers (**b**), grazers (**c**), detritivores (**d**), planktivores (**e**), micro-invertivores (**f**), macro-invertivores (**g**), piscivores (**h**) and piscivores (**i**) in community log-biomass for 832 reef slope sites from around the world. Grey dots are reef-level observations; blue dots are

a 0.1 log-kg interval moving average; GAM fits are represented by mean (solid black line) and 95% confidence intervals (dashed line) across the full data range. Mean model fits between initial reserve biomass and recovered log-biomass (vertical dotted lines) were scaled relative to their values at  $0.1B_0$  to characterize reef fish functional responses in Fig. 2.

**Extended Data Figure 7 | GAM functional returns with uncertainty.**

Average relative reef fish functional returns in log-biomass across the range from collapsed to recovered given the GAM fits in Fig. 2d; lines are GAM fits for

log-biomass per functional group relative to their average biomasses at marine reserve age zero (estimated initial log-biomass) in Fig. 1; dashed lines are approximate 95% confidence intervals. Data include 832 individual reefs.


**Extended Data Figure 8 | Nuisance parameter residual error plots.**

**a–c**, Joint Bayesian hierarchical recovery model nuisance parameter absolute residuals and residual histograms for percentage of hard coral cover (**a**), having been collected on an atoll (**b**) and average productivity in  $\text{kg C ha}^{-1} \text{ day}^{-1}$  (**c**).

Dashed red lines indicate weak linear trends in absolute residuals showing no heteroscedasticity was present; blue solid lines show a normal probability distribution fit to the residuals, demonstrating appropriate normal sub-model fit.

Extended Data Table 1 | DIC-based model selection for individual nuisance parameter sub-models

Model	Hard coral (%)	Depth (m)	Reserve size (km <sup>2</sup> )	Productivity (C kg/ha/day)	DIC
M1	Linear	-	-	-	1763.4
M2	Polynomial (2)	-	-	-	1764.5
<b>M3</b>	<b>Polynomial (3)</b>	-	-	-	<b>1762.8</b>
<b>M4</b>	-	<b>Linear</b>	-	-	<b>1769.4</b>
M5	-	Polynomial (2)	-	-	1773.0
M6	-	Polynomial (3)	-	-	1772.8
M7	-	-	Linear	-	1772.9
<b>M8</b>	-	-	<b>Polynomial (2)</b>	-	<b>1765.2</b>
M9	-	-	Polynomial (3)	-	1773.1
M10	-	-	-	Linear	1766.3
M11	-	-	-	Polynomial (2)	1763.6
<b>M12</b>	-	-	-	<b>Polynomial (3)</b>	<b>1754.4</b>

Joint Bayesian hierarchical recovery model selection for covariates thought to influence standing biomass. Candidate models include linear, second-order polynomial (2) and third-order polynomial (3) models for each nuisance parameter fit individually (that is, other nuisance parameters absent from full model). Models M1–M12 were used to select the best model form for each parameter given the lowest deviance information criteria (DIC) value (bold) for each.

Extended Data Table 2 | DIC-based model selection for combined nuisance parameter sub-models

Model	Hard coral (%)	Depth (m)	Reserve size (km <sup>2</sup> )	Productivity (C kg/ha/day)	Atoll	DIC	ΔDIC
M13	Polynomial (3)	Polynomial (2)	Polynomial (2)	Polynomial (3)	-	1753.6	9.7
M14	-	Polynomial (2)	Polynomial (2)	Polynomial (3)	-	1757.2	13.3
M15	Polynomial (3)	-	Polynomial (2)	Polynomial (3)	-	1750.8	6.9
M16	Polynomial (3)	Polynomial (2)	-	Polynomial (3)	-	1754.3	10.4
M17	Polynomial (3)	Polynomial (2)	Polynomial (2)	-	-	1762.4	18.5
M18	-	-	Polynomial (2)	Polynomial (3)	-	1759.8	15.9
M19	-	Polynomial (2)	-	Polynomial (3)	-	1760.2	16.3
M20	-	Polynomial (2)	Polynomial (2)	-	-	1769.7	25.8
M21	Polynomial (3)	-	-	Polynomial (3)	-	1747.3	3.3
M22	Polynomial (3)	-	Polynomial (2)	-	-	1764.1	20.2
M23	Polynomial (3)	Polynomial (2)	-	-	-	1758.5	14.6
M24	Polynomial (3)	Polynomial (2)	Polynomial (2)	Polynomial (3)	1	1748.5	4.6
M25	-	Polynomial (2)	Polynomial (2)	Polynomial (3)	1	1751.4	7.5
M26	Polynomial (3)	-	Polynomial (2)	Polynomial (3)	1	1746.2	2.3
M27	Polynomial (3)	Polynomial (2)	-	Polynomial (3)	1	1749.0	5.1
M28	Polynomial (3)	Polynomial (2)	Polynomial (2)	-	1	1758.4	14.5
M29	-	-	Polynomial (2)	Polynomial (3)	1	1755.5	11.6
M30	-	Polynomial (2)	-	Polynomial (3)	1	1755.2	11.3
M31	-	Polynomial (2)	Polynomial (2)	-	1	1765.4	21.5
<b>M32</b>	<b>Polynomial (3)</b>	-	-	<b>Polynomial (3)</b>	<b>1</b>	<b>1743.9</b>	<b>0.0</b>
M33	Polynomial (3)	-	Polynomial (2)	-	1	1758.8	14.9
M34	Polynomial (3)	Polynomial (2)	-	-	1	1753.6	9.7

Joint Bayesian hierarchical recovery model selection for covariates thought to influence standing biomass. Candidate models include varying combinations of linear, second-order polynomial (2) and third-order polynomial (3) models for each nuisance parameter selected as the lowest DIC-valued model in Extended Data Table 1. Models M13–M34 were used to select parameters included in the final model given the lowest DIC value (**bold**). Atoll 1 indicates atoll offset was included in the model.